AD-HOC WIRELESS SENSOR POSITIONING IN HAZARDOUS AREAS

R. Mautz [a] *, W. Y. Ochieng [b], H. Ingensand [a]

[a]Swiss Federal Institute of Technology, Institute of Geodesy and Photogrammetry, Wolfgang-Pauli-Str. 15,
CH-8093 Zurich - mautz@geod.baug.ethz.ch
[b]Centre for Transport Studies, Department of Civil and Environmental Engineering
Imperial College London, London SW7 2AZ, United Kingdom-（w.ochieng）@imperial.ac.uk

Commission I, ThS-1

KEY WORDS: Wireless Positioning, Ad-hoc Sensor Networks, Hazard Monitoring, Network Adjustment, Volcano Watch

ABSTRACT:

This paper investigates the capability of GNSS aided smart sensor network positioning based on Wireless Local Area Network (WLAN) signals incorporating access points, to monitor 3D deformation associated with volcanic activity and other comparable hazardous events. While a small number of GNSS receivers provide the coordinate and time references, low-cost low-power wireless sensor nodes with ranging capabilities create a dense positioning network. The simulations presented in this paper are based on a novel positioning algorithm that is robust with respect to errors in the inter-node range measurements. Based on a fine digital surface model of the Sakurajima volcano, various scenarios for setting up a monitoring network are assessed. The optimal number and location of nodes is determined for a future deployment of such a wireless sensor network. Results show that 2D positioning accuracy is to be expected in the magnitude of the mean range observation error. However, the crucial height component exhibits twice the error variance compared to the horizontal component. This is due to the poor geometric configuration in relation to height that is intrinsic to a ground based network.

1. INTRODUCTION

Many of the world's volcanoes that erupt, experience significant pre-eruption surface deformation. Internal magma pressure makes the surface bulge upwards and outwards. Thus, precise monitoring of surface deformation has the potential to contribute significantly to the realisation of a predictive capability of volcanic eruption. In particular, eruption source depth and evolution time can be estimated from surface deformation. The scale of this deformation is typically centimetric to decimetric over tens of square kilometres and over periods of weeks. Horizontal displacements show typically a radial pattern of movement of up to 10 cm with the displacement of the vertical components in the range of 4 to 6 cm per year (Wadge et al., 2005). Furthermore, the paper demonstrated that SAR interferometry images could be used to detect displacements of 70 to 90 mm uplift. However, data rates of typically 35 days are too slow for an early warning system.

In addition to the use of precise positioning and timing information to facilitate direct monitoring of deformation, the positioning function is vital for spatio-temporal referencing of the relevant multiple and complementary data types for volcano monitoring (e.g., seismicity, ground surface deformation, geothermal, gravity, and geomagnetic). This approach is particularly useful for enhanced risk assessment and early warning of volcanic eruptions. In architectural terms the monitoring network is an array of distributed intelligent nodes (sensor motes), consisting of low-cost, commercially available, and off-the-shelf components (as far as possible) with built-in local memory and intelligence, with self-configuration, communication, interaction and cooperative networking capabilities. The nodes should be able to identify the type, intensity, and location of the parameters being measured, and collaborate in an inter-nodal manner with each other to perform distributed sensing for event confirmation and significance.

Janssen (2002) has shown that geodynamic applications such as volcano deformation monitoring, require a dense spatial coverage of sensor stations. Although the requirement for centimetre level accuracy points to the need for GNSS carrier phase measurements, the need to keep costs down (both in terms of technical complexity and power consumption), precludes the exclusive need to build expensive carrier phase GNSS chips into all WLAN (Drescher et al. 2008). Hence, a compromise scenario is to have both types of nodes, some equipped with WLAN as well as carrier phase chips that are used for absolute coordinate and time referencing but with the majority of nodes with only WLAN communication and ranging capabilities.

The limited GNSS aiding proposed should enable WLAN positioning to deliver centimetre level positioning (and high accuracy timing) both in terms of error calibration and temporal synchronisation. In this case the sensors equipped with GNSS chips calculate their positions in a higher reference frame with high accuracy, and serve as anchor (= control or reference) points for the monitoring network. The communication function of the network should enable the exchange of the data required for positioning within the monitoring network. This includes communication between the sensors, and between the WLAN nodes and GNSS reference stations. This should enable GNSS aiding to take place but accommodate the flexibility of allowing the WLAN nodes to position themselves exploiting inter-node distance

measurements. With a high density of WLAN nodes, the inter-node distances between volcanic activity sensors are expected to be short thereby enhancing positioning accuracy.

Such a monitoring system requires multiple key features including construction of the hardware that fulfil the requirements in terms of size, battery life and robustness, the extraction of ranges (distances) between sensor nodes, appropriate supporting network communications, protocol development, optimal routing and positioning. Currently various research activities are underway globally to study the feasibility of smart sensing for environmental applications. This study addresses specifically the position function and characterises the performance of a novel high positioning algorithm using simulated range measurements at the Sakurajima volcano in Japan.

2. POSITIONING STRATEGY

2.1 WLAN POSITIONING

WLAN (Wireless Local Area Network) has the potential to deliver sub-decimetre level positioning. Besides WLAN, alternative methods of extracting ranges between two devices are currently in development. Brodin et al. (2005), use the time of flight between two Bluetooth transceivers to derive inter-node ranges. A two-way ranging technique is used to cancel the clock bias and obtain accurate range between two devices. Certain short range ultrasound based positioning systems also reach cm-level accuracy (Priyantha, 2005). However, in hazardous environments with relatively large areas to cover, such methods are not practical. Research is also underway on the use of ultra wideband (Gezici et al, 2005) or even based on Teraherz technology for positioning.

RSSI (Received Signal Strength Indicator) or cell-ID methods are not used for deformation monitoring due to their unreliability and inaccuracy. Here, the Time of Arrival (ToA) method is preferred, where the time delay is used to derive the distances between nodes if there is a direct line of sight. To date there has not been a practical demonstration of the capability of any of the current approaches to deliver centimetre level positioning in a continuous and reliable manner as required for monitoring of deformation associated with volcanos. However, research has shown that there is every likelihood that this will be the case in the near future.

A significant part of a high accuracy positioning system to support deformation monitoring is the positioning algorithm used to generate position, timing and derivative data. This paper presents a novel positioning algorithm (explained briefly in this section) for use with high quality range measurements. The algorithm allows for the determination of network sensor node coordinates based on a set of range measurements under certain circumstances and is independent of the type of signal used.

2.2 POSITIONING ALGORITHM

The local 3D positioning algorithm presented in this paper takes into account the weaknesses of current wireless ad-hoc positioning methods and algorithms, including the absence of quality and integrity indicators for the positioning results and performs well even in the presence of high variances in range measurements.

The positioning strategy can be broken down into two phases:

1. Creation of a rigid structure: The key issue for anchor free positioning is to find a globally rigid graph, or in other words, a structure of nodes and ranges which has only one unique embedding, but still can be rotated, translated and reflected. In 3D, the smallest graph consists of five fully connected nodes in general position. If such an initial cluster passes statistical tests, additional vertices are added consecutively using a verified multilateration technique.
2. Transformation of the cluster(s) into a reference coordinate system: If the local cluster contains at least four vertices that are also anchor nodes in a reference system, then the cluster is eligible for a transformation into that particular coordinate system. The process flow of the overall positioning strategy is illustrated in Figure 1.
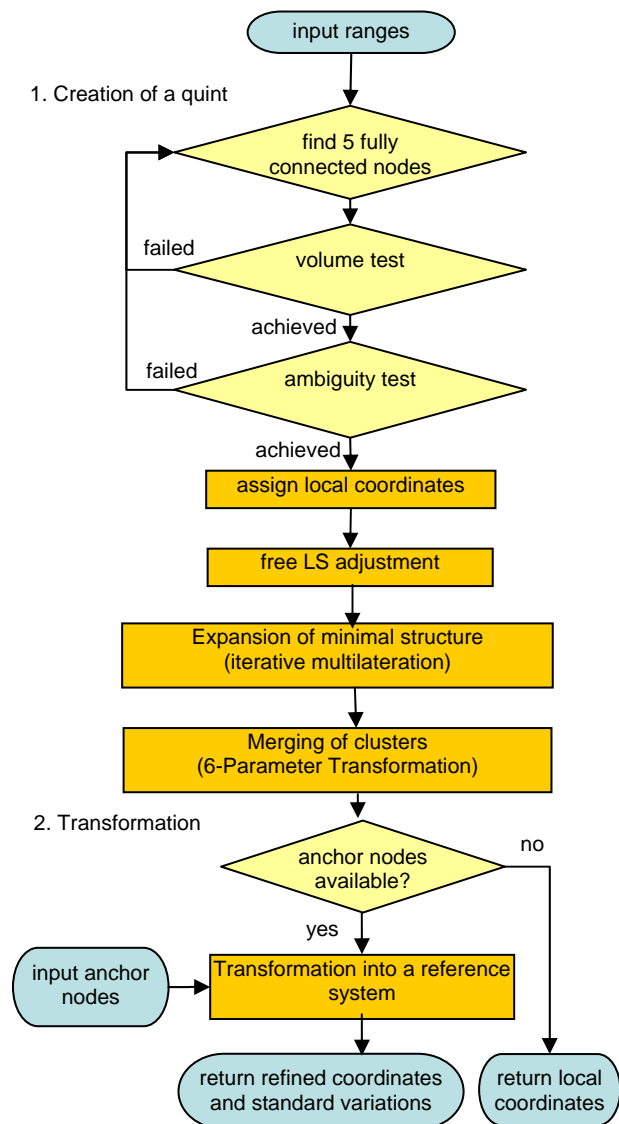

Fig. 1 Positioning algorithm, which does not require any initial approximate coordinates.

2.2.1 Computation of a rigid structure

The creation of a cluster aims to compute unique positions of vertices in a local coordinate system that can be transformed to a global system by translation, rotation and reflection. A

straightforward method to determine the position of an object based on simultaneous range measurements from three stations located at known sites is called trilateration. Thomas and Ros (2005) provide fast algebraic and numeric algorithms for trilateration in robotics. Coope (2000) shows that the effect of errors in the range measurements can be particularly severe when the trilaterated point is located close to the base plane or the three known stations are nearly aligned. Moore et al. (2004) show that there is a high probability of incorrect realisations of a 2D-graph when the measurements are noisy. For 3D-trilateration the system of observation equations of the form

$$(x - x_i)^2 + (y - y_i)^2 + (z - z_i)^2 = r_i^2 \qquad (1)$$

has to be solved, where $\mathbf{P}_i = (x_i, y_i, z_i)$, $i = 1, 2, 3$ are the known coordinates of station i, and r_i is the range measurement associated with it. This problem is equivalent to finding the intersection point(s) of 3 spheres in R^3. Such an interpretation allows an easy geometric proof that usually there will be two points of intersection, because, if $\mathbf{P}$ is a solution to the problem, then clearly the reflection of $\mathbf{P}$ in the plane defined by the 3 given points will also be a solution. The ambiguity can only be solved if the location of $\mathbf{P}$ is known approximately a priori. But this may not be the case in automatic ad-hoc networks.

However, as long as there are only 4 points involved, the flip ambiguity does not affect the inner structure of the general tetrahedron which is spanned by the base plane and the trilaterated point. The forth point is added to the network by 3D-tilateration thereby arbitrarily choosing one of the two solutions and discarding the other.

As soon as a 5th node is added to the cluster by trilateration from the points in the base plane 1, 2 and 3, the ambiguity problem does matter, as there are two different embeddings. As shown in Figure 2, nodes 4 and 5 could be on either the same side of the base plane or on opposite sides.
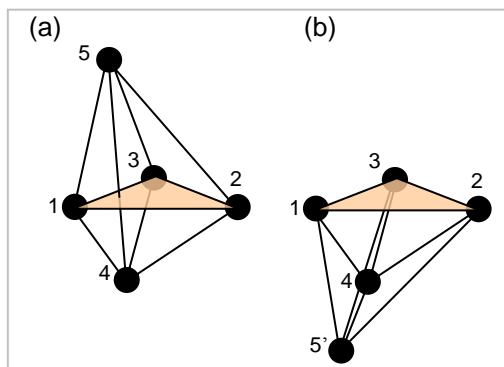

Fig. 2 (a) Quintilateral, (b) a version where node 5 has been mirrored at the base plane

If the distance between nodes 4 and 5 is also measured, this graph is referred to as a 'quintilateral' or in short a 'quint' since all 5 nodes are fully linked by range measurements to each other. Only the additional range measurement r_{45} between nodes 4 and 5 can disambiguate between these two embeddings. As can be seen in the example in Figure 2, r_{45} is significantly longer than the corresponding range in the reflected case $r_{45'}$, which means that if range r_{45} is available, the correct

embedding can be selected. Consequently, such a quint is rigid in 3D, assuming the nodes are not in a singular position.

However, there are geometric constellations where the ambiguity cannot be solved by the redundant range r_{45}, because the difference between the computed distances d_{45} and $d_{45'}$ is of the same magnitude as the range measurement error. In order to decide which of the two embeddings is correct, we compare the computed distances d_{45} and $d_{45'}$ with the measured distance r_{45}. In some cases the differences between the measured and the calculated distances $\Delta_{45} = |r_{45} - d_{45}|$ and $\Delta_{45'} = |r_{45} - d_{45'}|$ may both be very small. Assuming a mean error of the range measurement r_{45}, say 10%, both differences Δ_{45} and $\Delta_{45'}$ are likely to pass the statistical test of their null hypotheses, which means that both could be a result of noise. Consequently, the range r_{45} does not disambiguate between both embeddings.

The best way to deal with this problem is to reject such unstable point formations. It is better not to use a non-robust quint than rely on a structure with incorrect internal flips. It is crucial to ensure a correct embedding for several reasons. Firstly, the displacement caused by an incorrect flip can be large. Secondly, these errors have a negative affect on the expansion of the structure when additional vertices are added later. Thirdly, and most importantly, incorrect flips in a network are hardly to be eliminated by applying geodetic network adjustment. Adjustment algorithms are usually based on iterative local optimisation techniques. Local optimisation however, follows the gradient of a multidimensional objective function – which means that it is not possible to get out of a local sub-optimum. Unfortunately, incorrect flips reflect such local optimums where local optimisation algorithms are likely to converge to. In order to overcome false flips, globally operating optimisation techniques would have to be used, which are computationally expensive for ad-hoc sensor network positioning.

When a quint is verified to be robust and not affected by a false flip, the next task is the expansion of the minimal rigid structure. The remaining nodes are added to the quintilateral (as a rigid structure) consecutively using 3D-multilateration from four or more stations. 'Multilateration' is basically a trilateration technique, where the new node is initially determined from three stations at a time. The remaining distance measurements are then again used to disambiguate between two different embeddings and to verify the initial computation. Multilateration allows redundant determination of the nodes. The resulting coordinate differences provide essential information to detect false range measurements, e.g. due to multipath effects.

However, there is again a high probability of incorrect folding of a graph when the measurements are noisy. For instance, if a new node is multilaterated from points located closely to one plane and the ranges are affected by errors, a flip ambiguity may occur due to the mirroring effect of that plane. These incorrect graph realisations need to be avoided by identifying weak tetrahedrons with volumes smaller than a threshold which is driven by the estimated noise in the ranges. Only tetrahedrons that have passed the test on robustness are further considered or otherwise discarded. This step again eliminates the mirroring ambiguity of nodes added to a rigid structure and improves the accuracy measures. Once a node's position is determined, it serves as an anchor point for the determination of further unknown nodes. This way, starting from the initial quintilateral the position information iteratively spreads through the whole network.

The trilateration and multilateration problem considered so far solves for one single unknown point at a time. The sequential accumulation of nodes by multilateration is known as iterative multilateration (Savvides, 2001). However, this technique is very sensitive to measurement noise. Initially, small errors accumulate quickly while expanding the network. Since the scenario we aim for is a large pure distance network with multiple unknown nodes and only a few known anchor nodes, the propagation of errors must be minimised as much as possible. In this case, geodetic network adjustment is an essential tool to evenly distribute the errors that have been accumulated during iterative multilateration. Network adjustment provides coordinate estimates of several unknown nodes thereby improving the reliability of the quality indicators as determined a posteriori. Although Least Squares (LS) adjustment is a powerful tool for the positioning task, one should be aware of the following issues:

a) The observation equations (1) are non-linear, but the adjustment is based on linear equations. The standard least-squares adjustment uses the Gauss-Newton method to iteratively achieve a solution. The iteration can only converge and provide the global solution for the unknown coordinates under the assumption that good quality approximation values for the unknowns are provided initially. Bad initial values due to flip ambiguities may cause the algorithm to diverge or converge into a sub-optimal local minimum. Additionally, side effects due to linearisation may also contribute to divergence.

b) Outlier observations distort the network but they cannot be isolated by performing a least-squares adjustment and analysing the residuals. Thus, outliers need to be removed in a separate analysis before the network is adjusted.

Both issues are accommodated by performing the anchor free start-up functionality based on multilateration, since it provides the essential approximate coordinates to enable network adjustment.

While performing simulations on the anchor free start-up, results show that only a fraction of vertices can become a member of one single cluster. The remaining vertices are likely to make up their own clusters which may or may not be connected to neighbouring clusters. In case two clusters share a sufficient number of vertices and/or range observations between them, they can be merged using an over-determined 3 dimensional 6-parameter transformation.

As this step is concluded by a free minimally-constrained least-squares adjustment, it is possible to assess the internal consistency of the measurements. The quality indicators of a free adjustment reflect only errors of the measurements without taking into account errors as a result of inaccurate anchor coordinates.

2.2.2   Transformation into a reference coordinate system

The outcome of clusterisation is a cluster of nodes with coordinates and their variances in a local system. Most applications require the network nodes to be tied in a coordinate system of a higher order. With a minimum availability of three anchor nodes, the local coordinates can be transformed into the relevant target system. Four nodes are necessary to solve for the folding ambiguity between two solutions. This can be achieved by a 3D-Cartesian coordinate transformation. A closed form solution for the determination of transformation parameters using the 3D-Helmert transformation is given by Horn (1987).

Subsequent to the transformation, a fully constraint LS network adjustment is performed that permits all of the available anchor nodes and all range measurements to be processed together in order to refine all approximate positions simultaneously. Additionally, the mean error in the coordinates is reported by a confidence ellipsoid for each node.

A more elaborate discussion of the positioning algorithm and details of the mathematical background are presented in Mautz et al. (2007).

3.   OPTIMISED NETWORK SET UP FOR VOLCANO SAKURAJIMA

Sakurajima is an active volcano and a former island (now connected to the mainland) of the same name in Kagoshima Prefecture in Kyūshū, Japan. It is a composite volcano with the summit split into three peaks; its highest peak rises to 1'117 metres above sea level.

The volcano is extremely active erupting almost constantly. Thousands of small explosions occur each year, throwing ash to heights of up to a few kilometres above the mountain. Monitoring of the volcano for predictions of large eruptions is particularly important due to its location in a densely populated area, with the city of Kagoshima's 600,000 residents just a few kilometres from the volcano.

Several institutions are involved in monitoring Sakurajima, including the Sakurajima Volcano Observatory (where data are captured by levelling, EDM and GPS) and Kagoshima University (which uses EDM and GPS). Additionally Landsat 7 images are analysed. However, a dense network of location aware nodes are still to be deployed. This section uses a Digital Surface Model (DSM) to simulate such a network and assesses the performance that could be achieved.

3.1 The Digital Surface Model

The network positioning analysis is based on a 10 m by 10 m reference DSM of the central parts of volcano Sakurajima comprising an area of 2 km by 2.5 km. A 3D view of the data is shown in Figure 3.
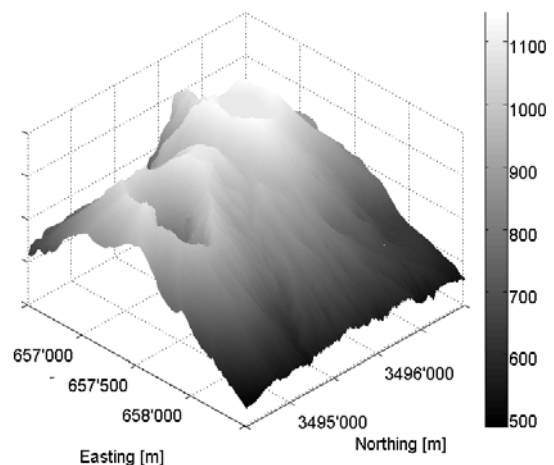

Fig. 3 Lateral View of Sakurajima Mountain based on a 10 m grid

In order to establish a useful network of sensors with positional awareness for Mount Sakurajima, several scenarios were simulated and assessed. The main driver for successful positioning in a sensor network is the geometry of the network, i.e. the locations of the nodes. Other key factors are the total number of nodes, number of anchors (i.e. reference) nodes, maximum range length and the mean error of the range measurements. Based on the positioning algorithm detailed in section 2, the performance of such a network can be quantified. Such a study supports a future real network implementation in general – not in particular for Mount Sakurajima.

3.2 Various Simulation Scenarios

In a first scenario 400 nodes were deployed on a 100 m grid. The assumption was made that the radio links are restricted to a maximum of 500 m assuming the usage of omnidirectional antennas and direct line of sight for WLAN signals in the 2.4 GHz band. Since the precise TOA ranging method requires direct line of sight, all observations with obstructed views were not considered. As a result, the network according to Figure 4 did not have the required density for positioning.

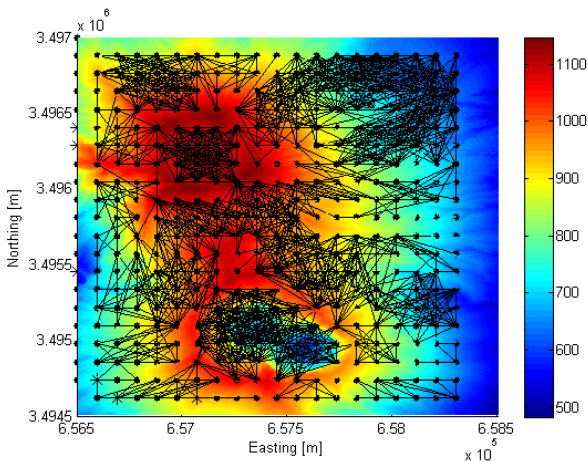Fig. 5 Optimised positions of the 400 nodes. All 5024 lines of sight with less than 500 m are shown.

Fig. 4 Original positions of 400 nodes on a 100 m by 125 m grid. All 1838 lines of sight with less than 500 m are shown.

In a second attempt the locations of the nodes were optimised for a maximum of line-of-sights using a heuristic global optimisation scheme, see Figure 5. The inter-nodal connectivity (i.e. the density of the network) is 3 times higher with 5024 ranges. In this case it was possible to compute the coordinates of all nodes in the network.

In another experiment the radio range, i.e. the maximal range observation between nodes was varied in a series between 200 m and 500 m. Figure 6 shows that the critical bound is at 350 m. The number of ranges to neighbours that the average node is able to observe is directly proportional to the maximal ranging distance, see Figure 7.

Another important parameter for a network configuration is the fraction of anchor nodes, i.e. the number of GPS reference stations. Results show that the minimum number for a 3D Helmert transformation of 3 reference points is not sufficient. Even the minimum number for our positioning algorithm of 5 reference stations does not mean that all nodes participate in the cluster with the anchor nodes. Deploying 5 anchors, not all
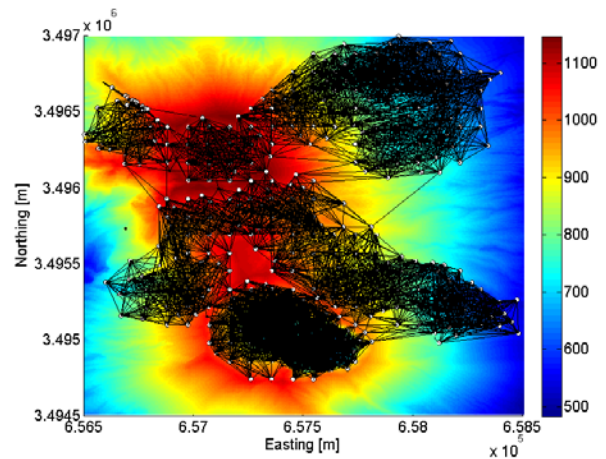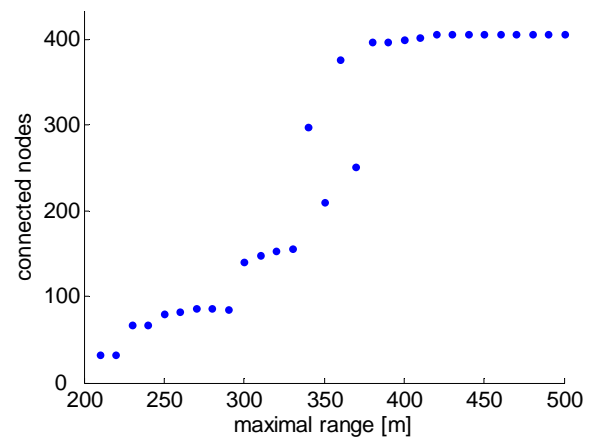

Fig. 6 Maximum radio range between nodes versus the number of 3D positions that can be determined precisely.
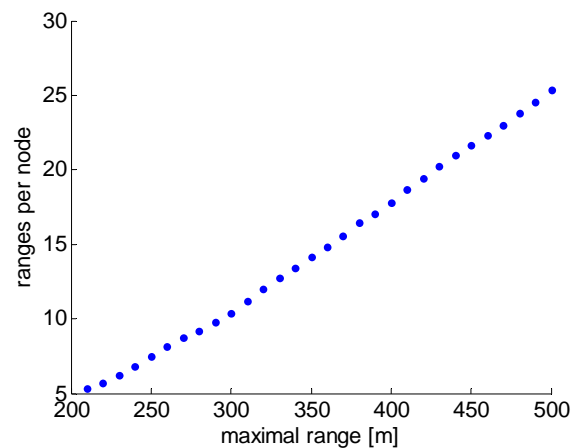

Fig. 7 Maximum radio range versus the average number of successful range measurements for each node.

nodes become part of the main cluster, see Table 1. In order to solve that problem, the number of anchors must be increased. Alternatively, the inter node connectivity can be enlarged.

Number of anchors	Anchor fraction	Number of located nodes	Number of ranges
3	0.8 %	3	3
5	1.2 %	191	3556
10	2.5 %	354	4553
15	3.8 %	371	4874
20	5.0 %	400	5024

Table 1 Success in precise positioning of network nodes in dependency of the number anchor nodes. The network size is 400 nodes.

The most problematic parameter in wireless positioning is the ranging accuracy, since the technology of precise ranging has not yet reached the level that most applications would need. According to Figure 8, the mean error (white noise) of the range observations was varied between 0 m and 1 m. Typically, the positional errors can be expected in the size of the range errors. Other factors, such as the network density, geometry, etc. also have an influence on the position errors. Since this is a simulation, we have the opportunity to compare the results with the true positions for a network with perfect ranges. At high noise levels, the estimated errors tend to be smaller than the true deviations – this effect is caused by undetected cases of folding errors, because a wrong embedding is not sensitive to error propagation.
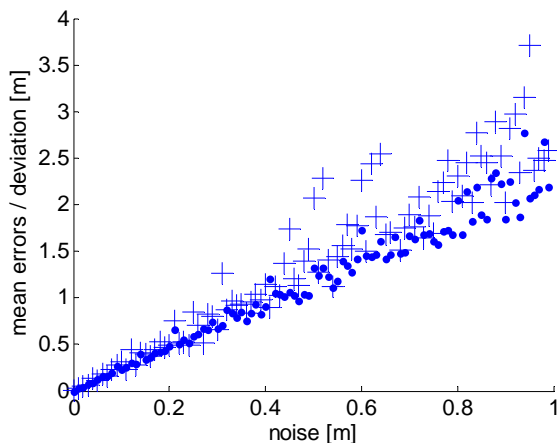

Fig. 8 Mean errors in the range measurements versus the mean position errors (·) and the deviations from "truth" (+).

One last observation – but nevertheless important – is that the errors of the height component are 2-3 times higher than the horizontal components, see Figure 9. This is a result of all nodes being deployed on the surface causing an unfavourable geometry for height determination.
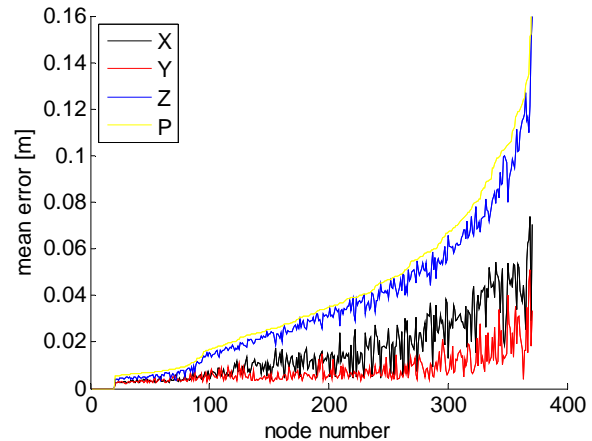

Fig. 9 Mean errors of the X- Y- and Z-components sorted by the mean position errors (P) of the wireless nodes.

4. CONCLUSIONS

This paper has shown that the implementation of a wireless deformation monitoring system is feasible if the current problem of extracting precise ranging is solved. The requirement to have direct line of sights between stations can be solved by locating the nodes for optimal directs sights. The number of required nodes depends on the transmission range. The required fraction of GNSS enabled reference nodes will be around 10%, depending on the network density.

REFERENCES

Brodin, G., Cooper, J., Kemp, A., Le, T.S., Walsh, D., Ochieng, W.Y., Mautz, R., 2005. A High Accuracy Bluetooth Ranging and Positioning System, *Proceedings of National NavigationConference NAV05*, The Royal Institute of Navigation, 1–3 November 2005, London.

Coope I., 2000. Reliable computation of the points of intersection of n spheres in n-space, *ANZIAM Journal*, Vol. 42(E), pp. C461-477.

Drescher, R., Leinen, S., Becker, M., 2008. Volcano monitoring by a GPS based hybrid sensor system, *Schriftenreihe der Fachrichtung Geodäsie*, TU Darmstadt, No. 28, p. 23 – 36.

Gezici, S., Sahinoglu, Z., Molisch, A.F., Kobayashi, H., Poor, H.V., 2005. A Two-Step Time of Arrival Estmation Algorithm for Impulse Radio Ultra Wideband Systems. European Signal Processing Conference (EUSIPCO).

Horn, B., 1987. Closed-from solution of absolute orientation using unit quaternions, *Journal of Opt. Soc. Amer.*, Vol. A-4, pp. 629–642.

Janssen, V., Roberts, C., Rizos, C., Abidin, H.Z., 2002. Low-Cost GPS-Based Volcano Deformation Monitoring at Mt. Papandayan, Indonesia. *Journal of Volcanology and Geothermal Research*, 115(1-2), pp. 139-151. Web: http://www .gmat.unsw.edu.au/snap/publications/janssen_etal2002c.pdf

Mautz, R., Ochieng, W.Y., Brodin, G., Kemp, A., 2007. 3D Wireless Network Localization from Inconsistent Distance Observations, *Ad Hoc & Sensor Wireless Networks*, Vol. 3, No. 2–3, pp. 141–170.

Moore, D., Leonard, J., Rus, D., Teller, S., 2004. Robust distributed network localization with noisy range measurements, *Proceedings of the ACM Symposium on Networked Embedded Systems,* 2004.

Priyantha N. B., 2005. The Cricket Indoor Location System, PhD Thesis, Massachusetts Institute of Technology, 199 p.

Savvides, A., Han, C., Strivastava, M., 2001. Dynamic Fine-Grained Localization in Ad-hoc Networks of Sensors, *Proceedings of ACM SIGMOBILE 2001*, Italy, July 2001.

Thomas, F., Ros., L (2005): Revisiting Trilateration for Robot Localization, *IEEE Transactions on Robotics*, Vol. 21, No. 1, pp. 93-101.

Wadge, G., Achache, J., Ferretti, A., Francis, P.W., Morley, J., Muller, J-P., Murray, J.B., Prati, C., Rocca, F., Stevens, N.F., Upton, M. Williams, C.A., 1997. Volcano monitoring using interferometric SAR, *Earthnet Online*, ESA, http://earth.esa .int/workshops/ers97/papers/wadge/ (accessed 20 Feb. 2008).

ACKNOWLEDGEMENTS AND APPENDIX (OPTIONAL)

.